



CHORUS

This is the accepted manuscript made available via CHORUS. The article has been published as:

## Parameter estimation for complex thermal-fluid flows using approximate Bayesian computation

Jason D. Christopher, Nicholas T. Wimer, Caelan Lapointe, Torrey R. S. Hayden, Ian Grooms, Gregory B. Rieker, and Peter E. Hamlington

Phys. Rev. Fluids **3**, 104602 — Published 11 October 2018

DOI: [10.1103/PhysRevFluids.3.104602](https://doi.org/10.1103/PhysRevFluids.3.104602)

1 **Parameter Estimation for Complex Thermal-Fluid Flows Using Approximate**  
2 **Bayesian Computation**

3 Jason D. Christopher,<sup>1</sup> Nicholas T. Wimer,<sup>1</sup> Caelan Lapointe,<sup>1</sup> Torrey R. S.  
4 Hayden,<sup>1</sup> Ian Grooms,<sup>2</sup> Gregory B. Rieker,<sup>1</sup> and Peter E. Hamlington<sup>1,\*</sup>

5 <sup>1</sup>*Department of Mechanical Engineering,*  
6 *University of Colorado, Boulder, Colorado 80309*

7 <sup>2</sup>*Department of Applied Mathematics, University of Colorado, Boulder, Colorado 80309*

8 (Dated: August 24, 2018)

9 **Abstract**

10 Approximate Bayesian computation (ABC) is a data-driven technique that uses many low-cost numerical  
11 simulations to estimate unknown physical or model parameters (e.g., boundary conditions and material  
12 properties), as well as their uncertainties, given reference data from real-world experiments or higher-fidelity  
13 numerical simulations. In this study, ABC is used to estimate unknown parameters in complex thermal-fluid  
14 flows, and the technique is demonstrated on a periodically forced high-temperature jet and a steadily forced  
15 helium-air plume. In the first case, computational reference data are used to assess the accuracy of ABC  
16 when estimating the frequency, amplitude, and mean of the periodic velocity forcing at the jet inlet. These  
17 tests show that ABC provides accurate and reasonably certain estimates of inflow parameters even when  
18 the model simulations imperfectly represent the physics underlying the reference data. These tests also  
19 show that measurements far from the inlet can be used to perform the estimation, and that temperature  
20 measurements can be used to infer velocity inflow parameters. For the second case, ABC is used to estimate  
21 the inlet Richardson number and its uncertainty given experimental measurements of the Strouhal number  
22 within the plume. Once again, the approach is able to accurately estimate unknown parameters with  
23 relatively low uncertainty. As a result, ABC is shown to be a versatile technique for estimating unknown  
24 physical parameters when knowledge of a real-world system is limited or incomplete.

---

\* peh@colorado.edu

## 25 I. INTRODUCTION

26 Computational simulations are widely used to design and analyze systems involving complex  
27 thermal-fluid flows, from microscale heat transfer in thermal management devices to liquid propul-  
28 sion in heavy-lift rockets. Nearly all such simulations are intended to provide three-dimensional  
29 (3D) spatially and temporally resolved numerical solutions of physics-based governing equations  
30 for realistic geometries, boundary conditions, and material properties. Prior to making simulation-  
31 based design and operational decisions, however, computational accuracy must be demonstrated  
32 by validating against (typically experimental) reference data for realistic or canonical test cases.  
33 As simulation fidelity has improved over the past decade with the development of higher-order and  
34 geometry-resolving numerical techniques, as well as with the increasing use of petascale computing  
35 resources to achieve very fine spatial resolutions and improved physical realism, a long-standing  
36 difficulty in such validation efforts has come into sharper focus.

37 Namely: *Even if a simulation is able to solve physically-realistic governing equations with high*  
38 *accuracy, unavoidable uncertainties in real-world boundary conditions, material properties, and*  
39 *other parameters result in ambiguity as to whether the computational and real-world systems are*  
40 *actually equivalent.* That is, there are few assurances that discrepancies between computational  
41 and experimental results during a validation test are not simply due to limitations in the character-  
42 ization of the real-world system. Cases where knowledge of a real-world system is limited include  
43 experiments that were not originally intended for validation purposes, systems with limited access,  
44 or parameters that are difficult to measure directly [1].

45 In broad terms, this difficulty can be addressed by proposing distributions of likely parameter  
46 values, performing simulations with parameters sampled from those distributions to determine the  
47 spread of outcomes in a particular quantity of interest within the flow, and then using statistical  
48 inference to determine distributions for unknown parameter values [1–4]. This approach can, in  
49 principle, be attempted using full Bayesian analyses, which have recently gained popularity for  
50 parameter estimation in engineering applications [5–8]. However, in nearly all such analyses, the  
51 requisite components of Bayes’ theorem (specifically, the likelihood function) may be unknown  
52 or enormously costly to compute and, consequently, non-physics-based reduced-order surrogate  
53 models have often been used to sample the unknown parameter space [6, 7, 9–11]. Optimization  
54 techniques have also been used for parameter estimation (e.g., [12–16]), but these methods seek to  
55 provide single values of unknown parameters, with no intrinsic measure of uncertainty when using  
56 potentially imperfect computational models and real-world data.

57 In the present study, approximate Bayesian computation (ABC), a data-driven Bayesian tech-  
58 nique adopted from the biological and geophysical sciences, is used to estimate unknown parameters  
59 for complex, turbulent thermal-fluid flows. The power of ABC lies in the fact that far fewer simula-  
60 tions are required than in full Bayesian analyses since ABC does not require a likelihood function,  
61 thus permitting the use of physics-based models. Rather than attempting to match the reference  
62 data at all locations and times, as in full Bayesian analyses, the ABC method develops an approx-  
63 imate posterior distribution for unknown parameters through comparison of summary statistics  
64 from the reference data and model simulations. A wide variety of reference data can be used to  
65 drive the estimation, including measurements that are only indirectly related to parameters of in-  
66 terest. Because the technique naturally provides posterior distributions for unknown parameters,  
67 Bayesian confidence intervals can be obtained along with parameter estimates. Once parameter  
68 estimates are obtained, they can either be used in higher-fidelity numerical simulations of the same  
69 system, or they can be considered as part of the description of the real-world system itself (with  
70 appropriate uncertainty caveats).

71 This study is one of a growing number of efforts to use data-driven methods with either exper-  
72 imental or higher-fidelity computational reference data to improve accuracy and quantify uncer-  
73 tainty in turbulent flow simulations. For example, ensemble Kalman filtering (EnKF) approaches  
74 have been used to assimilate reference data in simulations [17–20] and to infer turbulence model  
75 discrepancies [21]. In such approaches, reference data are used to update the state of a simulation  
76 or parameters in the simulation as the simulation progresses. Generally, however, EnKF methods  
77 require extensive and high quality reference data to provide reliable state and parameter estimates.  
78 The maximum *a posteriori* (MAP) method has also been used to infer both parameter [22] and  
79 model [23] uncertainties. This method maximizes the posterior using either an analytical function  
80 or a Monte Carlo approach, but the analytical function used to represent the posterior (or the  
81 likelihood function) is often only known approximately, and the number of simulations required  
82 in even Markov chain Monte Carlo approaches can be enormous. Recently, the ABC method has  
83 been used to infer Arrhenius parameters for chemical kinetics rate coefficients in the context of  
84 combustion [24].

85 The present study is specifically targeted at problems for which the reference data are spatially  
86 and temporally sparse, statistical in nature, or otherwise lacking in sufficient detail to update the  
87 model simulations at all locations and times (precluding the use of EnKF methods) and for which  
88 the true posterior is either intractable or prohibitively expensive to compute (precluding the use of  
89 MAP methods). As a demonstration of ABC, this paper outlines the estimation of inflow boundary

90 conditions for two compressible turbulent flows: (i) a periodically forced high-temperature jet, and  
91 (ii) a weakly but steadily forced helium-air plume. Both cases are two-dimensional (2D), but are  
92 physically complex due to compressibility and the corresponding coupling between temperature,  
93 density, buoyancy, and forced advection. The first case is intended to demonstrate the utility and  
94 breadth of ABC by using computational reference data to estimate the frequency, amplitude, and  
95 mean of the forced inflow. Since these parameters and the underlying physical model are precisely  
96 known for the computational data, the success of the ABC approach can be quantified. The second  
97 case is a demonstration of ABC using experimental measurements in an engineering context.

98 It should be noted that the present study is focused on demonstrating the use of ABC for  
99 estimating *physical* parameters that are difficult to obtain for real-world systems, as opposed  
100 to calibrating *model* parameters used in reduced-order or engineering models of more complex  
101 phenomena. Such model parameter calibrations are also possible using ABC and are the subject  
102 of future research [25].

## 103 II. APPROXIMATE BAYESIAN COMPUTATION

104 The ABC framework is a relatively new approach for linking reference data to physical and  
105 model parameters [26–32]. It was first conceived by Rubin [33] and then subsequently applied by  
106 Pritchard *et al.* [34] to the study of population dynamics. Although the technique has traditionally  
107 been applied in biology [34–40], it has recently gained traction in geophysics [41–47], primarily for  
108 calibrating parameters in reduced-order models of complex phenomena. It has also been used  
109 recently in the context of chemical kinetics modeling for combustion [24].

110 From a fundamental perspective, the ABC method produces a posterior distribution of unknown  
111 parameters given some reference data. This occurs by comparing observations or summary statistics  
112 from the reference data to corresponding data or summary statistics from lower-cost physics-  
113 based ‘model’ simulations (e.g., simulations with coarse spatial resolutions or lower-order numerical  
114 schemes). The model simulations are repeated many times, with each simulation using parameters  
115 drawn from a prior distribution. The prior distribution is the best guess at the span of the unknown  
116 parameter space; it must be wide enough to contain the true parameter values, but narrow enough  
117 to keep the task computationally manageable. Parameter values are retained if the model data  
118 or summary statistics are similar to the reference observations. Once many such candidates are  
119 obtained, a posterior distribution is formed, providing estimates for the most likely parameter  
120 values as well as their uncertainties, given the reference data.

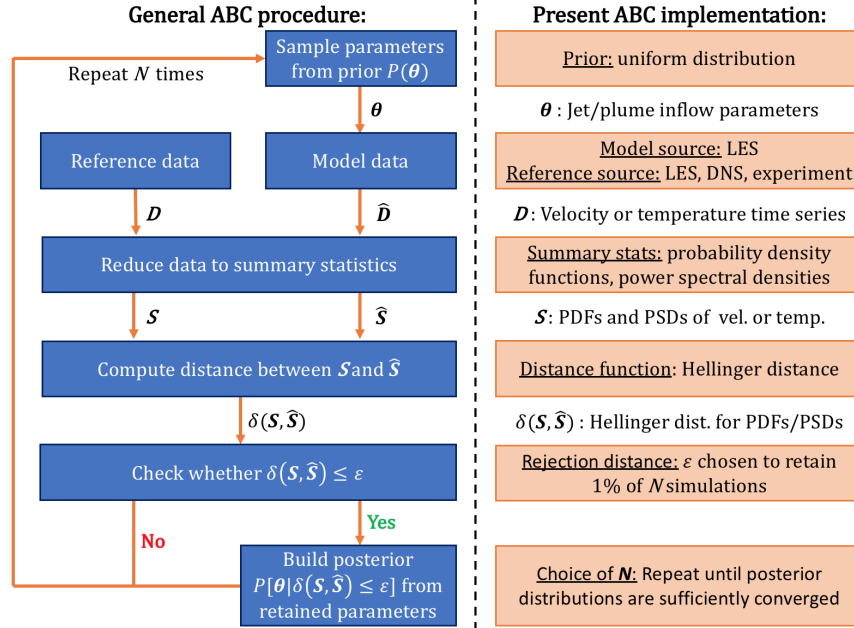


FIG. 1. [Color online] Schematic of the general ABC approach corresponding to Method D from Marjoram *et al.* [27], and of the specific ABC implementation used in the present study.

121 The specific ABC algorithm used in this work is Method D from Marjoram *et al.* [27]. Given  
 122 the summary statistic  $\mathcal{S}$  obtained from reference data  $\mathcal{D}$ , this algorithm involves the following  
 123 steps (see also the schematic in Figure 1):

- 124 1. Generate parameters  $\theta$  from the prior distribution  $P(\theta)$ .
- 125 2. Simulate approximate data  $\hat{\mathcal{D}}$  using parameters  $\theta$  and compute the approximate statistic  $\hat{\mathcal{S}}$ .
- 126 3. Calculate the distance  $\delta(\mathcal{S}, \hat{\mathcal{S}})$  between the reference,  $\mathcal{S}$ , and simulated,  $\hat{\mathcal{S}}$ , statistics.
- 127 4. Accept  $\theta$  if  $\delta(\mathcal{S}, \hat{\mathcal{S}}) \leq \varepsilon$  (where  $\varepsilon$  is the ‘rejection distance’) and build the posterior distri-  
 128 bution of accepted parameters, denoted  $P[\theta | \delta(\mathcal{S}, \hat{\mathcal{S}}) \leq \varepsilon]$ .
- 129 5. Return to step 1 and repeat a total of  $N$  times until a reasonable estimate is obtained for  
 130 the posterior distribution.

131 In general, the parameters  $\theta$ , data  $\mathcal{D}$  and  $\hat{\mathcal{D}}$ , and summary statistics  $\mathcal{S}$  and  $\hat{\mathcal{S}}$ , are multi-  
 132 dimensional and are correspondingly indicated by boldface notation.

133 In broad terms, the prior distribution is simply the initial guess for the values of the true  
 134 parameters. Greater confidence in the values of unknown parameters permits a more concentrated  
 135 prior distribution (e.g., a Gaussian instead of a uniform distribution). The only requirement on

136 the prior is that its range spans the true values of the unknown parameters. In many practical  
137 cases, a wide prior can be used initially to gain an approximate idea of the true parameter values,  
138 and then a narrower prior can be used to determine parameter values with greater precision.

139 The use of summary statistics is intended to reduce the overall computational cost of the pa-  
140 rameter estimation. Although it would be ideal to compare all of the available data  $\mathbf{D}$  to all of the  
141 simulation data  $\hat{\mathbf{D}}$ , this is typically a very high-dimensional problem and is not computationally  
142 feasible in general. Thus, instead, summary statistics are used. A key challenge in successfully  
143 implementing ABC is to identify relevant summary statistics that significantly reduce the dimen-  
144 sionality of the data, while still maintaining sufficient identifiability of unknown parameters [48].  
145 Examples of summary statistics include averages, standard deviations, probability distribution  
146 functions (PDFs), and power spectral densities (PSDs).

147 The choice of distance function is typically based on the form of the summary statistic. For  
148 example, the root mean square error can be used to compare spatial profiles of average quantities  
149 and the Hellinger distance [49] or Kullback-Leibler divergence [50] can be used to compare PDFs.  
150 The specific choice of rejection distance,  $\varepsilon$ , is typically determined by a balance between computa-  
151 tional cost and parameter estimate uncertainty. Smaller values of  $\varepsilon$  lead to higher rejection rates  
152 and reduced uncertainty in estimated parameter values [28], but also increase the number of model  
153 simulations necessary to generate a sufficiently converged posterior.

154 With respect to evaluating the success of the ABC parameter estimation, “accuracy” can be  
155 assessed either by comparing the approximate posteriors generated using ABC to the true poste-  
156 riors, or by comparing the estimated parameter values to the true parameter values, along with  
157 a measure of certainty in the estimated values. In the present study, the true posteriors are not  
158 known analytically and they are prohibitively expensive to compute numerically. As a result, the  
159 accuracy of the ABC approach is quantified here by computing 95% Bayesian confidence intervals  
160 (sometimes called credible intervals), denoted  $C_B$ , from the approximate parameter posteriors,  
161 then determining whether  $C_B$  contains the true parameter value. The ultimate measure of accu-  
162 racy in the present study is indicated by how closely a central tendency of the posterior (such as  
163 the mean) matches the true parameter value. The degree of certainty in the estimated parameter  
164 value is determined by the width of  $C_B$ , where narrower intervals indicate more certain parameter  
165 estimates.

166 Additional details on the specific choices for the prior, summary statistics, distance function,  
167 and rejection distances used in the present ABC implementation are outlined in the following  
168 sections, and are also summarized in Figure 1.

### 169 III. DEMONSTRATION OF ABC USING COMPUTATIONAL REFERENCE DATA

170 As a demonstration of ABC, inflow parameters for a periodically forced high-temperature tur-  
171 bulent buoyant jet [51–55] are estimated using computational reference data. This case is examined  
172 due to the simplicity of the geometry combined with the complexity of the high-temperature un-  
173 steady compressible flow physics. Large eddy and direct numerical simulations (LES and DNS,  
174 respectively) are used as reference data, and model simulations are performed using LES.

175 The use of computational reference data allows the success of ABC to be assessed when the  
176 physics underlying the reference data, as well as all system parameters, are known exactly. Three  
177 questions, in particular, are addressed: (*i*) How accurately can ABC estimate unknown parameters  
178 when the reference data physics are exactly reproduced by the model simulations? (*ii*) How accu-  
179 rately can ABC estimate unknown parameters using model simulations that imperfectly represent  
180 the physics of the reference case? (*iii*) How accurately can ABC estimate unknown parameters  
181 using reference data that are only indirectly connected to the parameters of interest?

182 The first question represents a ‘best case scenario’ where there is zero model error and is ex-  
183 amined using both model and reference data from LES. Despite the exact correspondence between  
184 the governing equations solved in the model and reference LES, however, the flow fields obtained  
185 from each of the simulations differ on a local and instantaneous basis due to the use of different  
186 random initial conditions. The second question pertains to a more realistic application of ABC  
187 where the physics governing the reference data are not exactly represented by the model simula-  
188 tions. This question is examined here using LES model simulations and DNS reference data, and  
189 is further addressed in Section IV using experimental reference data. The third question addresses  
190 the identifiability of unknown parameters using different types of reference data, and is exam-  
191 ined by performing ABC at different heights above the inlet using either velocity or temperature  
192 measurements.

193 It should be noted that the test where both the model and reference data are obtained from  
194 LES most closely resembles an observing system simulation experiment (OSSE), which is a common  
195 technique used for the validation of data assimilation methods [56, 57]. In the present context, the  
196 OSSE represented by this test allows the choices of prior, summary statistic, distance function, and  
197 rejection distance to be evaluated in the absence of model error. In this sense, these tests indicate  
198 whether the ABC approach can ever be expected to succeed, and to what extent. The following  
199 analysis illustrates that, even in such a ‘best case scenario’, the ABC parameter estimation does not  
200 perfectly recover the true parameter values due to the presence of stochasticity in the model and



201 reference data. That is, the model and reference data are never in perfect local and instantaneous  
202 agreement because each of the simulations are initialized with different random temperature fields  
203 (even when using identical boundary parameter values). Thus, the true parameter values are only  
204 ever recovered approximately, even when the governing equations used to generate the model and  
205 reference data are identical.

206 The test where the model data are obtained from LES and the reference data from DNS is  
207 intended to address a common concern when parameter estimation methods are evaluated using  
208 OSSEs. Namely, that assessments of the method are likely to be overly optimistic due to the exact  
209 correspondence between the physics and numerics underlying the model and reference simulations.  
210 This issue, sometimes referred to as an “inverse crime” [58, 59] or the “identical/fraternal twin  
211 problem” [60, 61], is typically resolved by using different models, for example with different dis-  
212 cretizations, numerics, or physics, for the generation of the reference data and for the parameter  
213 estimation. Here, the LES-DNS tests are intended to provide a more realistic assessment of the  
214 accuracy of the ABC method than the LES-LES tests, since both the grid resolution and underly-  
215 ing governing equations in the LES and DNS are different. The test using experimental reference  
216 data and LES model data in Section IV is similarly intended to enable a more realistic assessment  
217 of the accuracy of the ABC approach.

## 218 A. Physical and Numerical Setup

219 The reference buoyant jet has a sinusoidally varying inlet velocity with a frequency of 4 Hz,  
220 an amplitude of 0.2 m/s, and a mean of 0.5 m/s. The inflow velocity is spatially uniform across  
221 the inlet. The physical domain is  $1 \times 2$  m and the inlet is 0.1 m wide. The ambient and inlet  
222 temperatures are 300 K and 1700 K, respectively, resulting in substantial density differences and  
223 buoyancy-driven flow. Instantaneous fields of velocity magnitude (i.e., speed) and temperature are  
224 shown in Figure 2.

225 All of the computations were performed using the FireFoam solver [62] within OpenFOAM  
226 [63, 64]. The simulations were restricted to 2D to minimize computational cost, although the ABC  
227 method is equally applicable in 3D. For the LES, the compressible filtered Navier-Stokes equations  
228 were solved with second-order accuracy in space and time using the one-equation eddy viscosity  
229 model [65] for closure of sub-grid scale stresses. The LES domain was discretized using 61,088  
230 cells, with grid stretching in the vertical direction and two levels of refinement near the jet inlet.  
231 For the DNS computations, the compressible Navier-Stokes equations were solved in conjunction

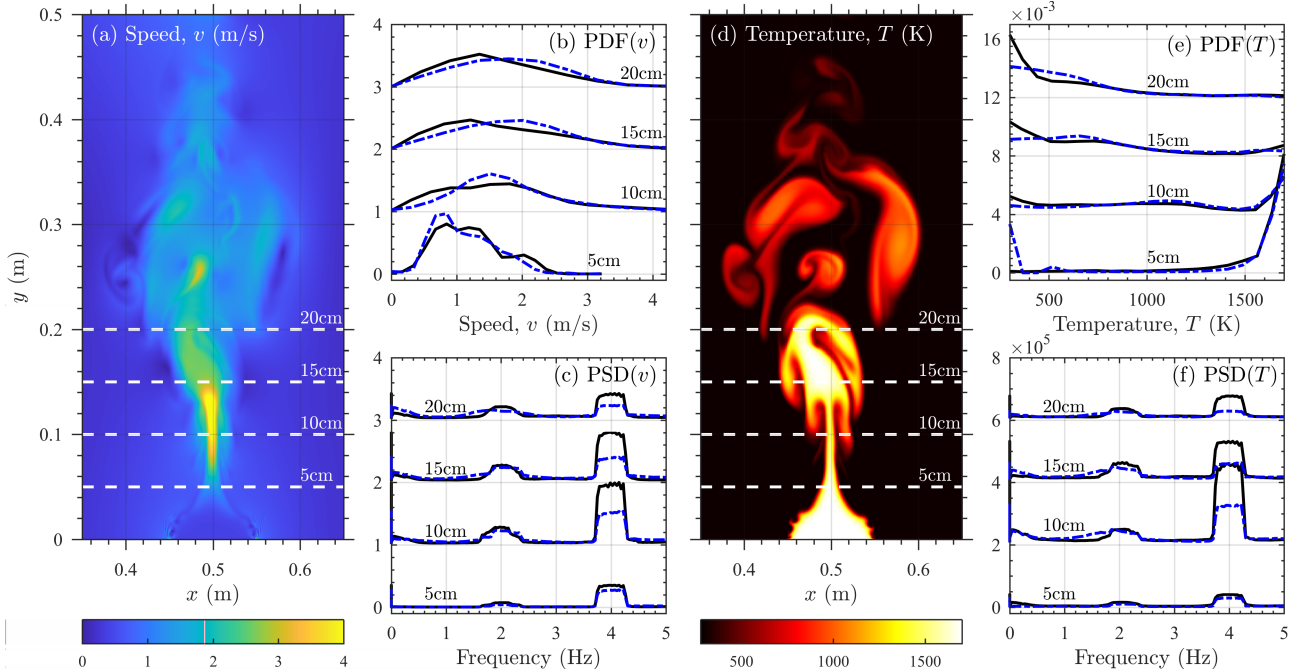


FIG. 2. [Color online] Representative fields of speed  $v$  (a) and temperature  $T$  (d) from DNS for the periodically forced turbulent buoyant jet. Panels (b) and (c) show reference probability density functions (PDFs) and power spectral densities (PSDs), respectively, of  $v$  at heights of 5, 10, 15, and 20 cm. PDFs and PSDs at different heights are shifted vertically for clarity. Panels (e) and (f) show corresponding PDFs and PSDs of  $T$ . Solid black lines in panels (b,c,e,f) show DNS reference data and dash-dot blue lines show LES reference data. PSDs are computed using Thomson’s multitaper estimate [68].

232 with the total energy equation at a high spatial resolution, again using a second-order accurate  
 233 numerical scheme in space and time. The DNS domain was discretized using 745,472 cells with  
 234 two levels of grid refinement, giving a grid that was over an order of magnitude larger than the  
 235 LES grid.

236 For both the LES and DNS, the ideal gas equation was used to relate state variables, and  
 237 fluid viscosity and specific heat varied with temperature according to the Sutherland model [66]  
 238 and JANAF tables [67], respectively. The LES and DNS numerical schemes were also the same,  
 239 with Crank-Nicolson time stepping and Gauss integration with linear interpolation for spatial  
 240 derivatives. Pressure-velocity coupling was accomplished using the PIMPLE algorithm, which  
 241 combines the pressure-implicit split-operator (PISO) and the semi-implicit method for pressure-  
 242 linked equations (SIMPLE). An adaptive time step was used to limit the maximum CFL condition  
 243 to 0.5 for the LES and 0.2 for the DNS.

## B. ABC Implementation

245 In this demonstration, ABC is used to estimate the frequency, amplitude, and mean of the  
 246 periodic forcing at the inlet of the buoyant jet given either LES or DNS reference data, with  
 247 model simulations from LES. The reference data consists of time series of speed or temperature  
 248 measured at nine heights above the inlet, ranging from roughly 0.5 mm up to 0.2 m. Time series  
 249 at each height were recorded over approximately 14 s after a 1 s initialization period, and PDFs  
 250 and PSDs were computed for each time series; these are the ABC summary statistics. The PSDs  
 251 were calculated using Thomson’s multitaper estimate [68, 69], which provides a robust estimate of  
 252 the PSD by reducing energy leakage across frequencies and reducing variance [70].

253 To ensure statistical convergence of the reference data, ensembles of 100 statistically independent  
 254 simulations were created using both LES and DNS. Each simulation had the same periodically  
 255 forced inflow at a frequency of 4 Hz, an amplitude of 0.2 m/s, and a mean of 0.5 m/s, but was  
 256 initialized using different stochastically generated temperature fields. The final reference data for  
 257 both the LES and DNS cases were then created by averaging the PDFs and PSDs for each of the  
 258 100 simulations in each ensemble, at each of the nine heights, giving the reference datasets shown,  
 259 for example, in Figure 2(b,c) for speed and in Figure 2(e,f) for temperature. Moreover, Figure 2  
 260 shows that the LES and DNS reference data are in reasonably good agreement.

261 Approximately  $10^4$  additional LES model cases were generated for the parameter estimation.  
 262 Each simulation was executed with a unique set of inlet parameters randomly sampled from prior  
 263 distributions for the frequency, amplitude, and mean of the sinusoidal velocity oscillations at the  
 264 inlet. The priors were uniform with bounds of 3.6–4.4 Hz for the frequency, 0.0–0.4 m/s for the  
 265 amplitude, and 0.0–1.0 m/s for the mean. Uniform priors were chosen to avoid the creation of  
 266 anomalous biases in the posterior distributions. The width of the priors for the amplitude and  
 267 mean were selected to be  $\pm 100\%$  the true parameter values, while the width of the frequency prior  
 268 is  $\pm 10\%$  the true value; it will be seen in the following that even with such a narrow frequency  
 269 prior, the posteriors go to zero at the edges of the prior for all heights. Although wider priors would  
 270 result in greater recovery of the edges of the posterior distributions, nearly all of the posteriors  
 271 obtained in this study display a pronounced maximum within the range of values present in the  
 272 priors. It should also be noted that the current priors are centered on the true values and that  
 273 off-centered priors could be formed, for example, by using widths that are  $[-100\%, +200\%]$  the  
 274 true values for the amplitude and mean and  $[-10\%, +20\%]$  for the frequency. However, once more,  
 275 the success of the ABC method will not be affected by the use of such off-centered priors provided

276 that the posteriors already display a distinct maximum within the bounds of the current centered  
277 priors, as is the case for nearly all of the tests performed here.

278 The Hellinger distance [49] was used to quantify the agreement between summary statistics from  
279 the reference and model data. Values for  $\varepsilon$  were chosen such that a fixed percentage of the tested  
280 parameters were retained in the final posterior [36, 39]. Parameter rejection was first performed  
281 using the Hellinger distance for the PSD, where  $\varepsilon$  was selected to reject 80% of all parameters  
282 tested. Subsequently, rejection was performed using the Hellinger distance for the PDF, with  $\varepsilon$   
283 chosen to reject 95% of the remaining parameters. With this sequential approach, only 1% of the  
284 parameters tested were included in the final posteriors.

### 285 C. Inflow Parameter Estimation Using LES Reference Data

286 Figures 3(a-f) show marginal posterior distributions for each inflow parameter using both speed  
287 and temperature reference data from LES at different heights. The posteriors are represented by  
288 Gaussian kernel estimations with bandwidths from Scott's normal reference rule [71]. As noted  
289 previously, these tests represent a best-case scenario for the ABC method where both the model  
290 and reference data physics are identical. Correspondingly, Figures 3(a,c,e) show that the true  
291 parameter values are captured by the ABC posteriors when using speed reference data from LES.  
292 In general, the uncertainty is smallest at locations close to the inlet, although reasonable estimates  
293 of the true parameters are still obtained at higher locations.

294 For the speed reference data, Figures 3(g,i,k) show that  $C_B$  is narrowest near the inlet when  
295 using LES reference data. This indicates that identifiability of the unknown parameters is greatest  
296 near the inlet when using the speed as reference data, although even higher in the domain it is still  
297 possible to estimate inflow parameters, albeit with less confidence. Figures 3(g,i,k) also show that  
298 mean values from the posteriors are in good agreement with the true values, particularly near the  
299 inlet for the amplitude and mean, and at all heights for the frequency.

300 The identifiability of unknown parameters using different measured quantities can be assessed  
301 by repeating the ABC procedure using PDFs and PSDs computed from temperature time series.  
302 Figure 3(b) shows that frequency predictions based on temperature reference data are all roughly  
303 centered on the true parameter value, and Figure 3(h) shows that the posterior means are in good  
304 agreement with the true value. The amplitude and mean posteriors in Figures 3(d,f) are centered  
305 around the true parameter values in the region from approximately 0.5 to 1.5 jet widths above the  
306 inlet. Below these heights, however, there is not enough variation in the temperature field to aid

307 in parameter estimation, given the uniform inflow temperature. Because the PDFs were nearly  
 308 identical at such low heights, the ABC procedure was modified such that 15% of the simulated  
 309 parameters were accepted based solely on the PSD comparison. Higher than 1.5 jet widths above  
 310 the inlet, the connection between the temperature field and the inlet velocity becomes weaker, re-  
 311 sulting in reduced identifiability of velocity boundary conditions using temperature measurements.  
 312 Despite these limitations, as shown in Figures 3(h,j,l), all parameters are predicted for all heights  
 313 within the  $C_B$  intervals for each posterior.

314 The amount of information gained about the unknown parameters during the ABC procedure  
 315 can be quantified using the Kullback-Leibler (KL) divergence [50] between the prior and posterior  
 316 distributions. Higher values of the KL divergence indicate that the posterior is significantly different  
 317 than the prior, while values close to zero indicate that the posterior is similar to the prior and that  
 318 little information about unknown parameters has been gained during the ABC procedure.

319 Figure 4 shows vertical profiles of the KL divergence for speed and temperature reference data  
 320 from LES, revealing that, in all cases, at least some information about the unknown parameters  
 321 is gained at nearly all locations within the domain. For the speed reference data in Figure 4(a),

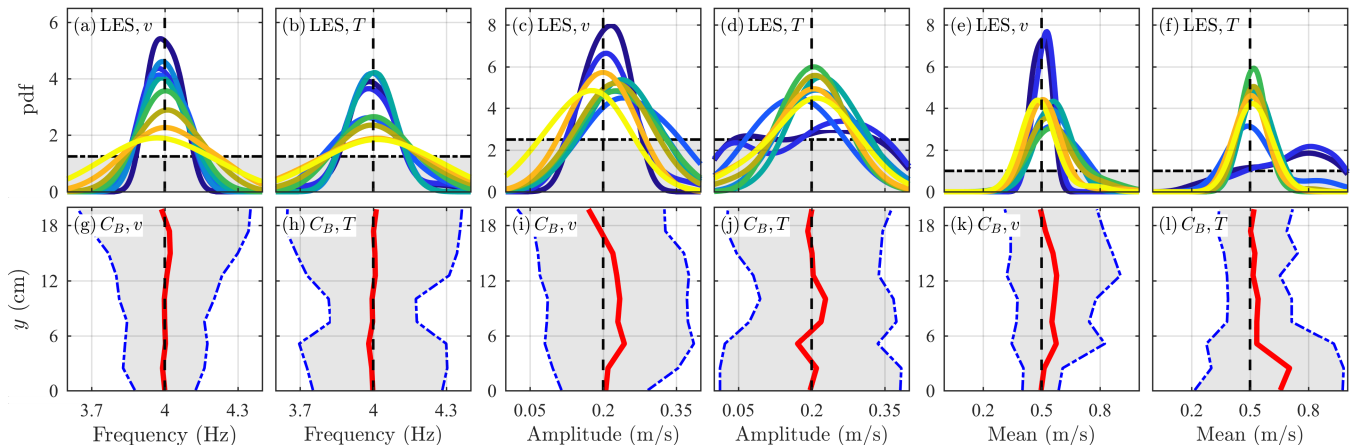


FIG. 3. [Color online] Top row: Marginal posterior distributions from ABC (visualized using Gaussian kernel estimation) for the frequency (a,b), amplitude (c,d), and mean (e,f) of the periodically forced turbulent buoyant jet using speed (a,c,e) and temperature (b,d,f) reference data from LES. Posteriors are calculated using measurements at heights from 0–20 cm (indicated by colors from blue to yellow). True parameter values are shown by vertical black dashed lines. Horizontal dash-dot lines and gray regions show the priors. Bottom row: Vertical profiles of 95% Bayesian confidence intervals,  $C_B$ , for the marginal posterior distributions in (a-f). Blue dash-dot lines and gray shading indicate the 95% Bayesian confidence regions, and the solid red lines show the mean values of the posteriors. True parameter values are shown by vertical black dashed lines.

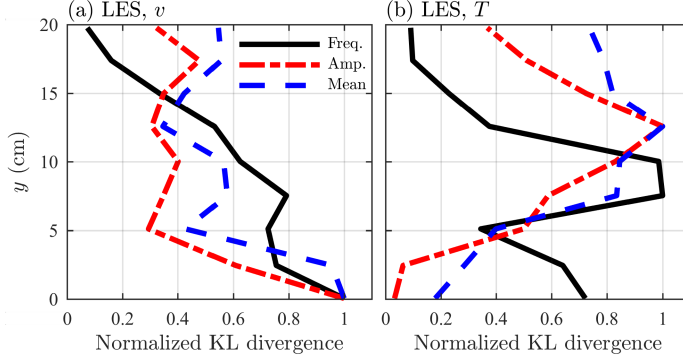


FIG. 4. [Color online] Vertical profiles of Kullback-Leibler (KL) divergences for the marginal posterior distributions in Figure 3 obtained using LES reference data. Divergences for the frequency (black solid lines), amplitude (red dash-dot lines), and mean (blue dashed lines) posteriors are shown for speed (a) and temperature (b) reference data. Each KL divergence vertical profile is normalized by its respective maximum value.

322 the greatest information about the unknown parameters is obtained near the jet inlet, and the  
 323 posteriors for the frequency generally provide more information higher in the domain than the  
 324 posteriors for the amplitude and mean. By contrast, for the temperature reference data in Figure  
 325 4(b), the greatest information is obtained higher in the domain, close to 10 cm (corresponding to  
 326 one jet width above the inlet). In general, only the temperature reference data near the jet inlet  
 327 fails to provide significant information regarding unknown parameter values.

#### 328 D. Inflow Parameter Estimation Using DNS Reference Data

329 As noted previously, evaluations of the ABC method based on tests where the same model is  
 330 used for the reference data and the parameter estimation (as in the LES-LES tests described in the  
 331 previous section) are likely to be overly optimistic. To address this issue, tests where the reference  
 332 data are generated by DNS and the parameter estimation is performed using LES have also been  
 333 carried out.

334 Figures 5(a-f) show marginal posterior distributions for each inflow parameter using both speed  
 335 and temperature reference data from DNS at different heights. As with the LES-LES results  
 336 shown in Figure 3, Figures 5(a,c,e) show that the true parameter values are captured by the ABC  
 337 posteriors when using speed reference data, with generally narrower posteriors close to the inlet.  
 338 This is also indicated by the variations of  $C_B$  in Figures 5(g,i,k), where it can be seen that  $C_B$  is  
 339 narrowest near the inlet when using speed reference data. The width of  $C_B$  consistently increases

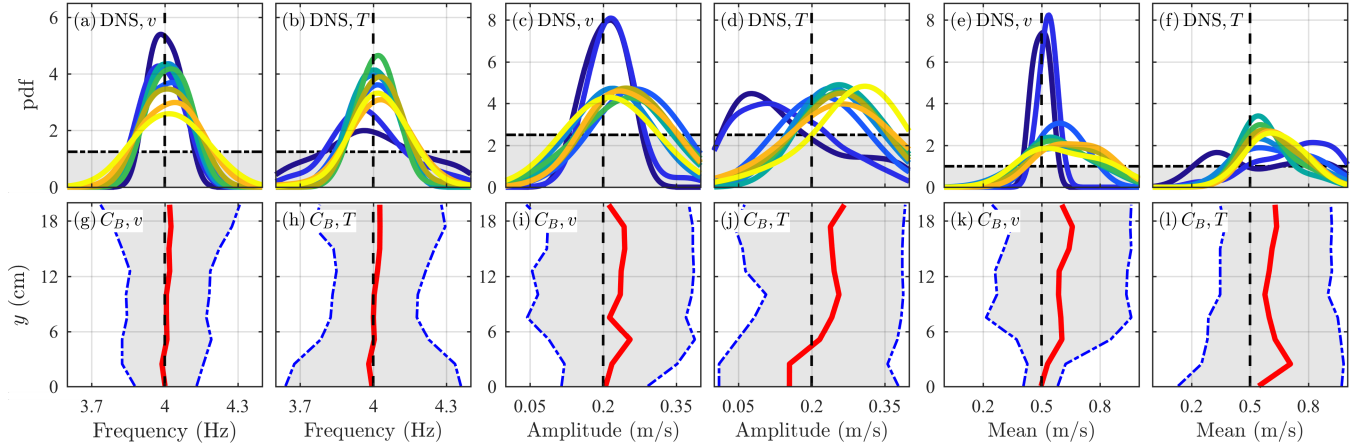


FIG. 5. [Color online] Top row: Marginal posterior distributions from ABC (visualized using Gaussian kernel estimation) for the frequency (a,b), amplitude (c,d), and mean (e,f) of the periodically forced turbulent buoyant jet using speed (a,c,e) and temperature (b,d,f) reference data from DNS. Posteriors are calculated using measurements at heights from 0–20 cm (indicated by colors from blue to yellow). True parameter values are shown by vertical black dashed lines. Horizontal dash-dot lines and gray regions show the priors. Bottom row: Vertical profiles of 95% Bayesian confidence intervals,  $C_B$ , for the marginal posterior distributions in (a-f). Blue dash-dot lines and gray shading indicate the 95% Bayesian confidence regions, and the solid red lines show the mean values of the posteriors. True parameter values are shown by vertical black dashed lines.

340 with height as the distance from the inlet increases. For each of the unknown parameters, posterior  
 341 means are generally close to the true parameter values.

342 For the temperature reference data from DNS, Figures 5(b,d,f) show that the marginal posterior  
 343 distributions once again capture the true parameter values with reasonable success. There is some  
 344 bias in the posteriors for the DNS reference data (particularly for the estimates of the amplitude  
 345 and mean), but the true parameter values are nevertheless contained within reasonably narrow  
 346 95% Bayesian confidence intervals. This is also shown in Figures 5(h,j,l), where  $C_B$  is widest for  
 347 the temperature-based DNS reference data near the inlet and narrowest roughly one jet width  
 348 above the inlet.

349 Vertical profiles of the KL divergence for the DNS reference data are shown in Figure 6. As with  
 350 the LES-LES results shown in Figure 4(a), Figure 6(a) shows that speed reference data from DNS  
 351 provides the greatest information about unknown parameters near the jet inlet, with the frequency  
 352 posteriors providing more information higher in the domain than the posteriors for the amplitude  
 353 and mean. For the temperature reference data in Figure 6(b), the greatest information is once  
 354 again obtained roughly one jet width above the inlet. In general, the trends shown in Figures 4

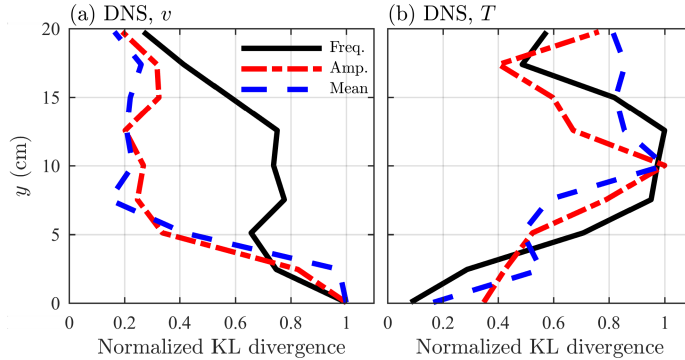


FIG. 6. [Color online] Vertical profiles of Kullback-Leibler (KL) divergences for the marginal posterior distributions in Figure 3 obtained using DNS reference data. Divergences for the frequency (black solid lines), amplitude (red dash-dot lines), and mean (blue dashed lines) posteriors are shown for speed (a) and temperature (b) reference data. Each KL divergence vertical profile is normalized by its respective maximum value.

355 and 6 are similar for the LES and DNS reference data, respectively.

356 Taken together, the results for the DNS reference data in Figures 5 and 6 indicate that the  
 357 ABC approach is successful even in non-overly-optimistic tests where the reference and model  
 358 data are significantly different. Overall, the parameter estimation is generally more accurate using  
 359 LES, as opposed to DNS, reference data, but this is unsurprising given the additional model error  
 360 introduced when using the DNS reference data. As a result, ABC is able to provide predictions  
 361 for unknown parameters using either exact or imperfect model simulations (as compared to the  
 362 reference data), and for locations that are indirectly related to the parameters of interest (i.e.,  
 363 using measurements at locations far from the inlet).

#### 364 IV. DEMONSTRATION OF ABC USING EXPERIMENTAL REFERENCE DATA

365 To demonstrate the utility of the ABC approach when the reference data are obtained from  
 366 an experiment, the ABC technique is next applied to a steadily forced planar plume for which  
 367 experimental data are available from Cetegen *et al.* [72]. In this experiment, a helium-air mixture  
 368 is weakly forced into 300 K ambient air, resulting in a natural oscillatory behavior of the plume.  
 369 By spanning a range of inflow conditions, Cetegen *et al.* [72] determined the empirical relation  
 370  $St = 0.55Ri^{0.45}$  between the Strouhal,  $St = fw/v_i$ , and Richardson,  $Ri = (1 - \rho_i/\rho_\infty)gw/v_i^2$ ,  
 371 numbers, where  $\rho_i$  is inlet density,  $\rho_\infty$  is ambient density,  $g$  is gravity,  $w$  is inlet width,  $v_i$  is inlet  
 372 velocity, and  $f$  is the frequency of the natural oscillation.



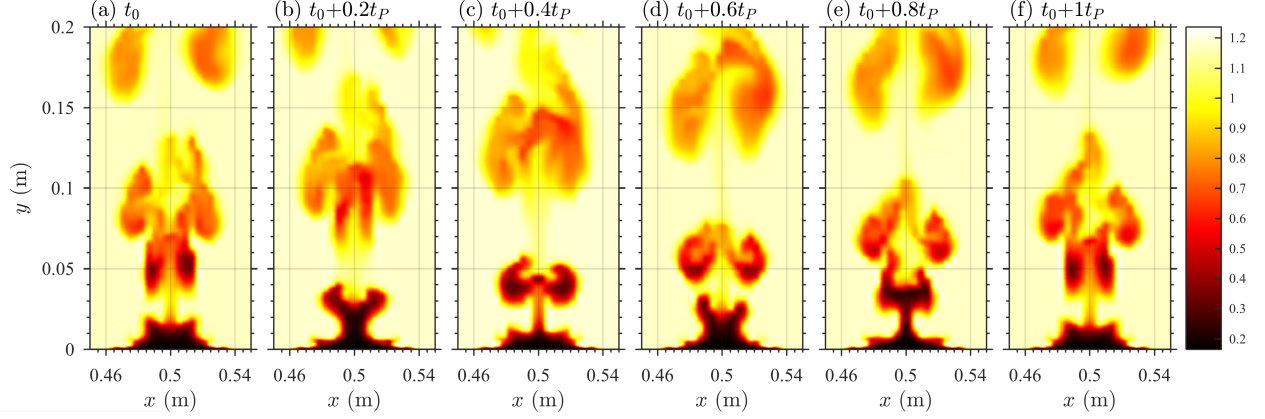


FIG. 7. [Color online] Representative 2D fields of density ( $\text{kg/m}^3$ ) from LES at six different times (a-f) for the steadily forced plume described in Section IV. The fields shown begin at an arbitrary time  $t_0$  late in the LES and are separated by a time interval spanning one complete period,  $t_P$  ( $t_P = 1/f = 0.22$  s).

373 In this demonstration, ABC is performed assuming that the oscillation frequency above the jet  
 374 inlet,  $f$ , has been measured experimentally and that the density of the inflow mixture,  $\rho_i/\rho_\infty$ , is  
 375 unknown (where  $\rho_i/\rho_\infty = 0.14$  for pure helium and 1 for pure air). All other properties of the  
 376 inflow, including  $v_i$  and  $w$ , are assumed to be known. This case thus serves as the first experimental  
 377 demonstration that ABC is able to accurately estimate unknown parameters in complex thermal-  
 378 fluid flows, while also providing measures of uncertainty in the parameter estimates.

379 The model simulations were once again performed using LES in FireFoam [62]. The plume had a  
 380 width of  $w = 0.07$  m and a steady uniform inflow velocity of  $v_i = 0.067$  m/s. The reference Strouhal  
 381 number was assumed to be  $St = 4$ , which is close to several values measured experimentally (see  
 382 Figure 8). The inlet width and velocity were held fixed for 100 LES runs while the inlet density  
 383 ratio varied from 0.14 to 0.6, corresponding to the published range of density ratios from [72]. The  
 384 lowest density ratio corresponds to pure helium while the upper value was found in [72] to be the  
 385 bounding case beyond which the characteristic natural oscillation was not observed. The Strouhal  
 386 number was obtained from the peak frequency in a fast Fourier transform of vertical velocity a  
 387 distance  $w$  above the inlet; this was the summary statistic. The distance function consisted of an  
 388 L1 error norm between reference and model peak frequencies, and  $\varepsilon$  was chosen to retain 20% of  
 389 the parameter values from the model simulations. The characteristic oscillation of the plume is  
 390 captured by the LES, as shown in Figure 7.

391 Figure 8 shows that the estimated value of  $Ri$  from ABC for  $St = 4$  agrees closely with the  
 392 experimental data. Additional tests for  $St = 2$  and 3 were also performed using  $v_i = 0.1$  m/s and  
 393  $0.15$  m/s, respectively. These different inlet velocities were necessary to span a range of  $Ri$  while

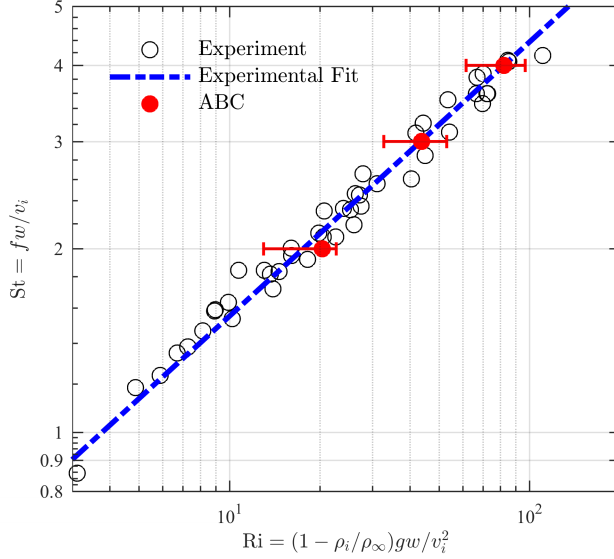


FIG. 8. [Color online] Relationship between Strouhal number  $St = fw/v_i$  and inlet Richardson number  $Ri = (1 - \rho_i/\rho_\infty)gw/v_i^2$  for the steadily forced helium-air plume. Experimental results from Cetegen *et al.* [72] are indicated by open circles, and the empirical fit  $St = 0.55Ri^{0.45}$  is shown as a blue dash-dot line. ABC results are indicated by filled red circles located at the mean  $Ri$  of the posterior distribution. Uncertainty bars show the minimum and maximum values of  $Ri$  in the posteriors.

394 constraining the physically allowable values of  $\rho_i/\rho_\infty$  to between 0.14 and 0.6. Once again, Figure  
 395 8 shows that ABC provides estimates of  $Ri$  that are in close agreement with experiments. As a  
 396 result, ABC correctly identifies the unknown  $Ri$  that would provide the desired natural oscillation  
 397 frequencies for known inlet velocity and width.

## 398 V. CONCLUSIONS

399 Approximate Bayesian computation (ABC) has been used to estimate unknown physical pa-  
 400 rameters in complex thermal-fluid flows. As a demonstration of the approach, ABC was used to  
 401 estimate the frequency, amplitude, and mean of the velocity inflow in a periodically forced turbu-  
 402 lent buoyant jet, as well as the inlet Richardson number for a steadily forced helium-air plume. In  
 403 the former case, computational reference data were used to drive the parameter estimation, while  
 404 in the latter case experimental reference data were used. For both cases, ABC provided accurate  
 405 estimates of unknown physical parameters even when the model simulations did not exactly match  
 406 the physics underlying the reference data (e.g., when using LES for the model simulations and  
 407 reference data from either DNS or experiments), and when the reference data were only indirectly

408 connected to the unknown parameters of interest (e.g., when using measurements distant from the  
409 jet and plume inlets, or when using temperature measurements to infer velocity inlet parameters).  
410 The primary impacts of using imperfect model simulations or only indirectly connected measure-  
411 ments were observed in the width of the Bayesian confidence intervals. As the physics of the model  
412 simulations more closely matched that of the reference data, and as the connection between the  
413 measurements and unknown parameters improved, the confidence intervals were found to become  
414 more narrow.

415 Although the present demonstration indicates that ABC provides accurate estimates of parame-  
416 ter values with relatively little uncertainty, there are many directions for future research. Different  
417 choices for the prior, summary statistic, distance function, and rejection distance can all poten-  
418 tially lead to slightly different parameter estimates. Further work is required to determine the  
419 specific effects of each of these choices on the accuracy and uncertainty of ABC. Markov chains  
420 can also be used to significantly reduce the cost of ABC by limiting the number of parameter  
421 values that are rejected, even for relatively small rejection distances [27]. Such approaches have  
422 become more popular in recent years, but have yet to be applied in the present context. Finally,  
423 the true power of ABC lies in its ability to predict unknown parameters in real-world systems, and  
424 future work will more deeply explore the use of experimental reference data to drive parameter  
425 estimates, particularly taking into account experimental uncertainty in the context of validation  
426 efforts for simulations of complex thermal-fluid problems. An important direction for future re-  
427 search is therefore to apply the ABC method to problems where the true parameter values are  
428 unknown.

## 429 ACKNOWLEDGMENTS

430 Helpful discussions with Mark Strobel, Aniruddha Upadhye, Colin Towery, Melvyn Branch, Jeff  
431 Anderson, and Daven Henze are gratefully acknowledged. N.T.W., C.L., and T.R.S.H. acknowledge  
432 gift support from the 3M Company. J.D.C. and G.B.R. were supported, in part, by NSF Award  
433 No. CBET 1454496. P.E.H. was supported, in part, by AFOSR Award Nos. FA9550-14-1-0273 and  
434 FA9550-17-1-0144. Computing resources were provided by DoD HPCMP under a Frontier project

435 award and by the Air Force Research Laboratory.

---

- 436 [1] W. L. Oberkampf and C. J. Roy. *Verification and validation in scientific computing*. Cambridge  
437 University Press, 2010.
- 438 [2] W. L. Oberkampf and T. Trucano. Validation methodology in computational fluid dynamics. In *Fluids*  
439 *2000 Conference and Exhibit*, page 2549, 2000.
- 440 [3] W. L. Oberkampf and T. G. Trucano. Verification and validation in computational fluid dynamics.  
441 *Progress in Aerospace Sciences*, 38(3):209–272, 2002.
- 442 [4] W. L. Oberkampf, T. G. Trucano, and C. Hirsch. Verification, validation, and predictive capability in  
443 computational engineering and physics. *Applied Mechanics Reviews*, 57(5):345–384, 2004.
- 444 [5] D. C. Estumano, F. C. Hamilton, M. J. Colaço, A. J. K. Leiroz, H. R. B. Orlande, R. N. Carvalho, and  
445 G. S. Dulikravich. Bayesian estimate of mass fraction of burned fuel in internal combustion engines  
446 using pressure measurements. *Engineering Optimization IV*, pages 997–1003, 2015.
- 447 [6] S. Mosbach, A. Braumann, P. L. W. Man, C. A. Kastner, G. P. E. Brownbridge, and M. Kraft. Iterative  
448 improvement of Bayesian parameter estimates for an engine model by means of experimental design.  
449 *Combustion and Flame*, 159(3):1303–1313, 2012.
- 450 [7] P. G. Constantine, Q. Wang, A. Doostan, and G. Iaccarino. A surrogate accelerated Bayesian inverse  
451 analysis of the HyShot II flight data. *AIAA Paper*, AIAA-2011-2037, 2011.
- 452 [8] I. Vrbik, R. Deardon, Z. Feng, A. Gardner, and J. Braun. Using individual-level models for infectious  
453 disease spread to model spatio-temporal combustion dynamics. *Bayesian Analysis*, 7(3):615–638, 2012.
- 454 [9] A. H. Elsheikh, I. Hoteit, and M. F. Wheeler. Efficient Bayesian inference of subsurface flow models  
455 using nested sampling and sparse polynomial chaos surrogates. *Computer Methods in Applied Mechanics*  
456 *and Engineering*, 269:515–537, 2014.
- 457 [10] S. Yeşilyurt and A. Patera. Surrogates for numerical simulations; optimization of eddy-promoter heat  
458 exchangers. *Computer Methods in Applied Mechanics and Engineering*, 121(1):231–257, 1995.
- 459 [11] L. Zeng, L. Shi, D. Zhang, and L. Wu. A sparse grid based Bayesian method for contaminant source  
460 identification. *Advances in Water Resources*, 37:1–9, 2012.
- 461 [12] A. G. Salinger, R. P. Pawlowski, J. N. Shadid, and B. G. van Bloemen Waanders. Computational  
462 analysis and optimization of a chemical vapor deposition reactor with large-scale computing. *Industrial*  
463 *& Engineering Chemistry Research*, 43(16):4612–4623, 2004.
- 464 [13] W. Jahn, G. Rein, and J. L. Torero. Forecasting fire dynamics using inverse computational fluid  
465 dynamics and tangent linearisation. *Advances in Engineering Software*, 47(1):114–126, 2012.
- 466 [14] H. Madsen. Parameter estimation in distributed hydrological catchment modelling using automatic  
467 calibration with multiple objectives. *Advances in Water Resources*, 26(2):205–216, 2003.
- 468 [15] S. Wang and X. Xu. Parameter estimation of internal thermal mass of building dynamic models using

- 469 genetic algorithm. *Energy Conversion and Management*, 47(13-14):1927–1941, 2006.
- 470 [16] E. Pemha and E. Ngo Nyobe. Genetic algorithm approach and experimental confirmation of a laser-  
471 based diagnostic technique for the local thermal turbulence in a hot wind tunnel jet. *Progress In  
472 Electromagnetics Research*, 28:325–350, 2011.
- 473 [17] H. Kato, A. Yoshizawa, G. Ueno, and S. Obayashi. A data assimilation methodology for reconstructing  
474 turbulent flows around aircraft. *Journal of Computational Physics*, 283:559–581, 2015.
- 475 [18] X. Gao, Y. Wang, N. Overton, M. Zupanski, and X. Tu. Data-Assimilated Computational Fluid  
476 Dynamics Modeling of Convection-Diffusion-Reaction Problems. *Journal of Computational Science*,  
477 21:38–59, 2018.
- 478 [19] J. Sousa, C. García-Sánchez, and C. Gorré. Improving urban flow predictions through data assimilation.  
479 *Building and Environment*, 132:282–290, 2018.
- 480 [20] J. R. Stroud and M. Katzfuss and C. K. Wikle. A Bayesian adaptive ensemble Kalman filter for  
481 sequential state and parameter estimation. *Monthly Weather Review*, 146(1):373–386, 2018.
- 482 [21] H. Xiao, J.-L. Wu, J.-X. Wang, R. Sun, and C. J. Roy. Quantifying and reducing model-form un-  
483 certainties in Reynolds-averaged Navier-Stokes simulations: A data-driven, physics-informed Bayesian  
484 approach. *Journal of Computational Physics*, 324:115–136, 2016.
- 485 [22] W. N. Edeling, M. Schmelzer, R. P. Dwight, and P. Cinnella. Bayesian Predictions of Reynolds-  
486 Averaged Navier?Stokes Uncertainties Using Maximum a Posteriori Estimates. *AIAA Journal*,  
487 56(5):2018–2029, 2018.
- 488 [23] A. P. Singh and K. Duraisamy. Using field inversion to quantify functional errors in turbulence closures.  
489 *Physics of Fluids*, 28:045110, 2016.
- 490 [24] M. Khalil and H. N. Najm. Probabilistic inference of reaction rate parameters from summary statistics.  
491 *Combustion Theory and Modeling*, DOI: 10.1080/13647830.2017.1370557, 2018.
- 492 [25] O. A. Doronina, J. D. Christopher, C. A. Z. Towery, P. E. Hamlington, and W. J. A. Dahm. Autonomic  
493 Closure for Turbulent Flows Using Approximate Bayesian Computation. *AIAA Paper*, AIAA-2018-  
494 0594, 2018.
- 495 [26] M. Sunnåker, A. G. Busetto, E. Numminen, J. Corander, M. Foll, and C. Dessimoz. Approximate  
496 Bayesian Computation. *PLoS Computational Biology*, 9(1):e1002803, 2013.
- 497 [27] P. Marjoram, J. Molitor, V. Plagnol, and S. Tavaré. Markov chain Monte Carlo without likelihoods.  
498 *Proceedings of the National Academy of Sciences*, 100(26):15324–15328, 2003.
- 499 [28] J. M. Marin, P. Pudlo, C. P. Robert, and R. J. Ryder. Approximate Bayesian computational methods.  
500 *Statistics and Computing*, 22(6):1167–1180, 2012.
- 501 [29] F. Hartig, J. M. Calabrese, B. Reineking, T. Wiegand, and A. Huth. Statistical inference for stochastic  
502 simulation models—theory and application. *Ecology Letters*, 14(8):816–827, 2011.
- 503 [30] A. B. Abdessalem, N. Dervilis, D. Wagg, and K. Worden. Model selection and parameter estima-  
504 tion in structural dynamics using approximate bayesian computation. *Mechanical Systems and Signal  
505 Processing*, 99:306–325, 2018.

- 506 [31] J. D. Christopher, N. T. Wimer, T. R. S. Hayden, C. Lapointe, I. Grooms, G. B. Rieker, and P. E. Ham-  
507 lington. Parameter Estimation for a Turbulent Buoyant Jet Using Approximate Bayesian Computation.  
508 *AIAA Paper*, AIAA-2017-0531, 2017.
- 509 [32] J. D. Christopher, C. Lapointe, N. T. Wimer, T. R. S. Hayden, I. Grooms, G. B. Rieker, and P. E. Ham-  
510 lington. Parameter Estimation for a Turbulent Buoyant Jet with Rotating Cylinder Using Approximate  
511 Bayesian Computation. *AIAA Paper*, AIAA-2017-3629, 2017.
- 512 [33] D. B. Rubin. Bayesianly justifiable and relevant frequency calculations for the applied statistician. *The*  
513 *Annals of Statistics*, 12(4):1151–1172, 1984.
- 514 [34] J. K. Pritchard, M. T. Seielstad, A. Perez-Lezaun, and M. W. Feldman. Population growth of human Y  
515 chromosomes: a study of Y chromosome microsatellites. *Molecular Biology and Evolution*, 16(12):1791–  
516 1798, 1999.
- 517 [35] S. Tavaré, D. J. Balding, R. C. Griffiths, and P. Donnelly. Inferring coalescence times from DNA  
518 sequence data. *Genetics*, 145(2):505–518, 1997.
- 519 [36] M. A. Beaumont, W. Zhang, and D. J. Balding. Approximate bayesian computation in population  
520 genetics. *Genetics*, 162(4):2025–2035, 2002.
- 521 [37] T. Toni, D. Welch, N. Strelkowa, A. Ipsen, and M. P. H. Stumpf. Approximate Bayesian computation  
522 scheme for parameter inference and model selection in dynamical systems. *Journal of the Royal Society*  
523 *Interface*, 6(31):187–202, 2009.
- 524 [38] K. Csilléry, M. G. B. Blum, O. E. Gaggiotti, and O. François. Approximate Bayesian computation  
525 (ABC) in practice. *Trends in Ecology & Evolution*, 25(7):410–418, 2010.
- 526 [39] M. A. Beaumont. Approximate bayesian computation in evolution and ecology. *Annual Review of*  
527 *Ecology, Evolution and Systematics*, 41(379-406):1, 2010.
- 528 [40] N. J. R. Fagundes, N. Ray, M. A. Beaumont, S. Neuenschwander, F. M. Salzano, S. L. Bonatto, and  
529 L. Excoffier. Statistical evaluation of alternative models of human evolution. *Proceedings of the National*  
530 *Academy of Sciences*, 104(45):17614–17619, 2007.
- 531 [41] J. A. Vrugt and M. Sadegh. Toward diagnostic model calibration and evaluation: Approximate Bayesian  
532 computation. *Water Resources Research*, 49(7):4335–4345, 2013.
- 533 [42] D. J. Nott, L. Marshall, and J. Brown. Generalized likelihood uncertainty estimation (GLUE) and  
534 approximate Bayesian computation: What’s the connection? *Water Resources Research*, 48(12), 2012.
- 535 [43] M. Sadegh and J. A. Vrugt. Bridging the gap between GLUE and formal statistical approaches:  
536 Approximate Bayesian computation. *Hydrology and Earth System Sciences*, 17(12), 2013.
- 537 [44] B. Olson. Stochastic weather generation with approximate bayesian computation. Master’s thesis,  
538 University of Colorado at Boulder, 2016.
- 539 [45] B. Olson and W. Kleiber. Approximate Bayesian computation methods for daily spatiotemporal pre-  
540 cipitation occurrence simulation. *Water Resources Research*, pages 1–21, 2017.
- 541 [46] D. D. Lucas, A. Gowardhan, P. Cameron-Smith, and R. L. Baskett. Impact of meteorological inflow  
542 uncertainty on tracer transport and source estimation in urban atmospheres. *Atmospheric Environment*,

- 543 143:120–132, 2016.
- 544 [47] J. Rohmer, M. Rousseau, A. Lemoine, R. Pedreros, J. Lambert, and A. Benki. Source characterisa-  
545 tion by mixing long-running tsunami wave numerical simulations and historical observations within a  
546 metamodel-aided ABC setting. *Stochastic Environmental Research and Risk Assessment*, pages 1–18.
- 547 [48] R. C. Smith. *Uncertainty quantification: theory, implementation, and applications*, volume 12. SIAM,  
548 2013.
- 549 [49] L. Le Cam and G. L. Yang. *Asymptotics in statistics: Some basic concepts*. Springer Science & Business  
550 Media, 2012.
- 551 [50] D. J. C. MacKay *Information Theory, Inference, and Learning Algorithms*. Cambridge University  
552 Press, 2003.
- 553 [51] S. C. Crow and F. H. Champagne. Orderly structure in jet turbulence. *Journal of Fluid Mechanics*,  
554 48(3):547–591, 1971.
- 555 [52] J. A. Lovett and S. R. Turns. Experiments on axisymmetrically pulsed turbulent jet flames. *AIAA*  
556 *Journal*, 28(1):38–46, 1990.
- 557 [53] R. B. Farrington and S. D. Claunch. Infrared imaging of large-amplitude, low-frequency disturbances  
558 on a planar jet. *AIAA journal*, 32(2):317–323, 1994.
- 559 [54] S. Marzouk, H. Mhiri, S. El Golli, G. Le Palec, and P. Bournot. Numerical study of momentum  
560 and heat transfer in a pulsed plane laminar jet. *International Journal of Heat and Mass Transfer*,  
561 46(22):4319–4334, 2003.
- 562 [55] W. Kriaa, H. B. Cheikh, H. Mhiri, G. Le Palec, and P. Bournot. Numerical study of free pulsed jet  
563 flow with variable density. *Energy Conversion and Management*, 49(5):1141–1155, 2008.
- 564 [56] C. P. Arnold Jr., C. H. Dey. Observing-systems simulation experiments: Past, present, and future.  
565 *Bulletin of the American Meteorological Society*, 67(6):687–695, 1986.
- 566 [57] M. Xue and M. Tong and K. K. Droegenmeier. An OSSE framework based on the ensemble square  
567 root Kalman filter for evaluating the impact of data from radar networks on thunderstorm analysis and  
568 forecasting. *Journal of Atmospheric and Oceanic Technology*, 23(1):46–66, 2006.
- 569 [58] J. Kaipio and E. Somersalo. Statistical and Computational Inverse Problems. *Applied Mathematical*  
570 *Series*, vol. 160, Springer, Berlin, 2004.
- 571 [59] J. Kaipio and E. Somersalo. Statistical inverse problems: Discretization, model reduction and inverse  
572 crimes. *Journal of Computational and Applied Mathematics*, 198:493–504, 2007.
- 573 [60] A. Stoffelen and G. J. Marseille and F. Bouttier and D. Vasiljevic and S. De Haan and C. Cardinali.  
574 ADM-Aeolus Doppler Wind Lidar Observing System Simulation Experiment. *Quarterly Journal of the*  
575 *Royal Meteorological Society*, 132:1927–1947, 2006.
- 576 [61] W. Lahoz and B. Khattatov and R. Menard (Eds.). Data Assimilation: Making Sense of Observations.  
577 Springer, Berlin, Heidelberg, 2010.
- 578 [62] Y. Wang, P. Chatterjee, and J. L. de Ris. Large eddy simulation of fire plumes. *Proceedings of the*  
579 *Combustion Institute*, 33(2):2473–2480, 2011.

- 580 [63] C. Greenshields. OpenFOAM | The OpenFOAM Foundation, March 2016.
- 581 [64] H. G. Weller, G. Tabor, H. Jasak, and C. Fureby. A tensorial approach to computational continuum  
582 mechanics using object-oriented techniques. *Computers in Physics*, 12(6):620–631, 1998.
- 583 [65] A. Yoshizawa. Statistical theory for compressible turbulent shear flows, with the application to subgrid  
584 modeling. *Physics of Fluids*, 29(7):2152–2164, 1986.
- 585 [66] W. Sutherland. LXXXV. A dynamical theory of diffusion for non-electrolytes and the molecular mass  
586 of albumin. *The London, Edinburgh, and Dublin Philosophical Magazine and Journal of Science*,  
587 9(54):781–785, 1905.
- 588 [67] D. R. Stull and H. Prophet. JANAF thermochemical tables. Technical report, DTIC Document, 1971.
- 589 [68] D. J. Thomson. Spectrum estimation and harmonic analysis. *Proceedings of the IEEE*, 70(9):1055–1096,  
590 1982.
- 591 [69] D. B. Percival and A. T. Walden. *Spectral analysis for physical applications*. Cambridge University  
592 Press, 1993.
- 593 [70] W. Van Drongelen. *Signal processing for neuroscientists: an introduction to the analysis of physiological*  
594 *signals*. Elsevier, 2006.
- 595 [71] D. W. Scott. On optimal and data-based histograms. *Biometrika*, 66(3):605–610, 1979.
- 596 [72] B. M. Cetegen, Y. Dong, and M. C. Soteriou. Experiments on stability and oscillatory behavior of  
597 planar buoyant plumes. *Physics of Fluids*, 10(7):1658–1665, 1998.